PERGAMON

Vision Research 41 (2001) 3649–3662

Vision Research

www.elsevier.com/locate/visres

Darkness filling-in: a neural model of darkness induction☆

Michael E. Rudd [a,*], Karl Frederick Arrington [b]

[a] *Department of Psychology, University of Washington, Box 351525, Seattle, WA 98195-1525, USA*
[b] *Arrington Research, Inc., Mesa, AZ 85206, USA*[1]

Received 14 February 2001; received in revised form 6 August 2001

Abstract

A model of darkness induction based on a neural filling-in mechanism is proposed. The model borrows principles from both Land's Retinex theory and BCS/FCS filling-in model of Grossberg and colleagues. The main novel assumption of the induction model is that darkness filling-in signals, which originate at luminance borders, are partially blocked when they try to cross other borders. The percentage of the filling-in signal that is blocked is proportional to the log luminance ratio across the border that does the blocking. The model is used to give a quantitative account of the data from a brightness matching experiment in which a decremental test disk was surrounded by two concentric rings. The luminances of the rings were independently varied to modulate the brightness of the test. Observers adjusted the luminance of a comparison disk surrounded by a single ring of higher luminance to match the test disk in brightness. © 2001 Published by Elsevier Science Ltd.

Keywords: Brightness; Brightness induction; Filling-in; Lightness; Retinex theory

1. Introduction

In the well-known simultaneous contrast illusion, two or more regions of an image that have identical physical luminances differ in brightness because of the differing luminances of their surrounds. For example, a middle gray paper appears darker when presented against a light background than it does when presented against a dark background. Wallach (1948) asked the closely related question: under what conditions will two regions surrounded by different backgrounds appear *equally* bright? To answer this question, he presented two disks, each having its own surround annulus (higher in luminance than the disk), side-by-side in an otherwise dark room. The luminance of one of the disks was adjusted as a function of its surround luminance to obtain a brightness match to the other disk, which had both a fixed luminance and fixed surround luminance. It was found that the brightnesses of the two disks matched whenever the *ratios* of their luminances to the luminances of their respective surrounds were equal. This result is known as *Wallach's ratio rule*. The ratio rule has since been shown to hold over a million-to-one range of illumination (Jacobsen & Gilchrist, 1988).

Wallach proposed a theoretical account of the ratio rule based on the principle of *brightness constancy*: surface brightness is invariant with respect to changes in illumination. This principle is closely related to the idea that brightness is the visual system's attempt to represent surface reflectance and discount the illuminant (Helmholtz, 1910/1925). According to the brightness constancy account, when the two disk-and-ring patterns have identical disk/surround luminance ratios, they are interpreted by the visual system as two identical configurations of surfaces illuminated by spotlights of different intensities. The presumed different illumination levels are 'discounted' in arriving at the psychophysical brightness match.

Although brightness constancy successfully explains why the two disks Wallach's display appear identical when their disk/surround ratios are equal, it *fails* to account for the equally important fact that the more

☆ The model has been presented earlier at professional conferences and published in the form of brief conference abstracts (Rudd & Arrington, 2000; Rudd, 2000).

* Correponding author. Tel.: +1-206-685-1572; fax: +1-206-685-3157.

E-mail address: mrudd@u.washington.edu (M.E. Rudd).

[1] http://www.ArringtonResearch.com.

0042-6989/01/$ - see front matter © 2001 Published by Elsevier Science Ltd.
PII: S0042-6989(01)00216-4

luminant surround ring appears brighter than the less luminant surround under these same conditions. If, as Wallach argued, the visual system interprets the two disk-and-ring configurations as two different objects having identical 'paint-jobs' but illuminated by different spotlights, then the *rings* on the two sides of the display should also appear equally bright, but they do not.

The brightnesses of *both* the disks and the rings in Wallach's display can be accounted for more parsimoniously on the basis of local border contrast. The disks look identical when the disk/annulus luminance ratios are the same because, under these conditions, the contrasts at the borders of the two disks are identical. The more luminant ring looks brighter than the less luminant ring because the contrast of its *outer* border is greater. However, it is clear from studies carried out with more complex displays that local contrast alone is not sufficient to account for brightness perception. In general, brightness also depends on nonlocal influences that are presumably based on the spatial integration of local contrast information.

A number of theoretical models of have been proposed to suggest how brightness might be computed on the basis of a neural process that integrates local luminance steps across space (Arend, 1985, 1994; Blake, 1985; Horn, 1974; Hurlbert, 1986; Land & McCann, 1971; Land, 1977, 1986). A common assumption of these models is that the visual system achieves brightness constancy by a neural computation involving a series of subprocesses or stages: (1) extraction of local luminance ratios at the locations of edges in the image; (2) spatial integration of these luminance ratios to reconstruct a map of relative surface reflectances; and (3) brightness anchoring, to relate the scale of relative surface reflectances to a common absolute brightness standard.

Most computational models assume that the luminance ratios computed by Stage 1 are *multiplied* across space to recover relative surface reflectances in Stage 2 (Arend, 1985, 1994; Blake, 1985; Gilchrist, Delman, & Jacobsen, 1983; Horn, 1974; Hurlbert, 1986; Land & McCann, 1971; Land, 1977, 1986; Whittle & Challands, 1969). Stage 3 is required to relate the scale of relative luminances to an absolute standard in order for the visual system to assign specific, as opposed to relative, brightness values (Cataliotti & Gilchrist, 1995).

This basic computational scheme for computing brightness, like the principle of brightness constancy itself, has become a standard working hypothesis within the psychophysical brightness literature. A number of recent psychophysical papers have addressed the problem of brightness anchoring (Stage 3 of the 'standard' model). Three different anchoring rules have been proposed in the literature. The first assumes that the space-average luminance is assigned the value 'gray' (Helson, 1943, 1964; Hurlbert, 1986; Hurlbert & Poggio, 1988; Judd, 1940; Land, 1986; Land, Hubel, Livingstone, Perry, & Burns, 1983). The second assumes that the highest luminance is assigned the value 'white' (Land, 1977; Land & McCann, 1971; Wallach, 1948, 1976). The third assumes that a gain control mechanism scales brightness according to a measure of space-averaged luminance variance (Brown & MacLeod, 1991, 1997). The results of most of the anchoring experiments have been interpreted as supporting the highest luminance rule (Bruno, 1992; Bruno, Bernardis, & Schirillo, 1997; Gelb, 1929; Li & Gilchrist, 1993; McCann, 1989, 1992; Schirillo & Shevell, 1993, 1996; Schirillo, 1999a,b).

The process of edge integration (Stage 2) has been investigated in much less detail. However, it is clear that under many stimulus conditions, the visual system does not *perfectly* integrate luminance steps across the entire visual image. The simultaneous contrast illusion, for example, depends on the fact that the contrast of the disk border has an inordinate influence on disk brightness. If all of the luminance steps in a simultaneous contrast display were perfectly integrated by the visual system, there would be no illusion. Instead, the ratios of the brightnesses of various regions within the figure would match the actual reflectance ratios of those regions.

One simple way of modeling the breakdown of perfect edge integration is to assume that edge integration declines with distance. A model of this type was proposed by Reid and Shapley (1988) to account for their data on contrast and assimilation. If edge integration declines with distance, then the luminance ratio at the immediate border of a region should exert a particularly important influence on the brightness of that region. Edges lying at a greater distance from the region could also affect its brightness, but they should have less of an influence than do nearby edges.

For purposes of exposition, it is useful to consider the two limiting cases of the distance-dependent edge integration hypothesis in which either: (1) edge integration declines very rapidly with spatial distance; or (2) edge integration does not decline with distance at all. In the limit of very rapid spatial falloff of integration, patch brightness should depend *only* on the local contrast at the immediate borders of the patch. A model of this type would account for simultaneous contrast and could be instantiated by a simple lateral inhibitory mechanism (Mach, 1865; Ratliff, 1965).

In the limit of long-distance edge integration, on the other hand, the visual system would be able to recover the overall pattern of relative reflectances in the image and would thus achieve brightness constancy to within a constant factor that depends on the anchor point, as in the computational models cited above.

The current study was designed to pit these two extreme models against one another and to collect data for the purpose of building a quantitative model to

account for expected compromises between complete edge integration and complete lack of edge integration. The experimental display consisted of a side-by-side pair of disk-and-ring patterns, as in Wallach's original experiment, but with a second, outer, surround added to the disk/annulus pair on the right (Fig. 1). The luminances of the two annuli on the right were constrained such that the luminance of the outer annulus was always either equal to or greater than the luminance of the inner annulus. The luminances of these two annuli were separately varied and the observer adjusted the luminance of the disk on the left to achieve a brightness match to disk on the right as a function of the luminances of its two surrounds.

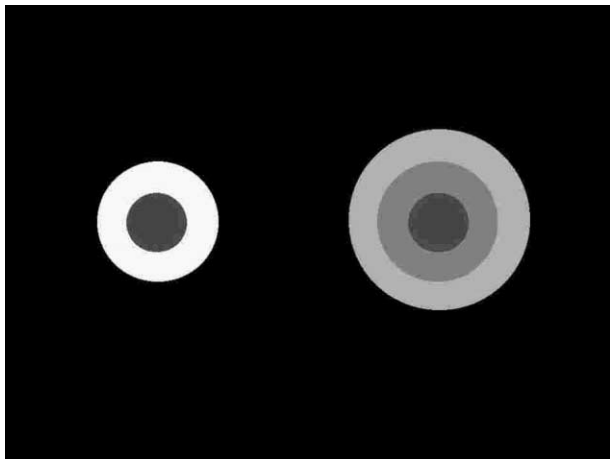

Fig. 1. Double-ring display. The test disk (*right*) was surrounded by two rings that were both of higher luminance than the test. The matching disk (*left*) was surrounded by a single ring that was of higher luminance than the matching disk. The luminances of the two rings surrounding the test were manipulated as the independent variables. The luminance of the outer ring was always either equal to or greater than that of the inner ring. To measure the magnitude of the darkness induction exerted on the test by increasing the intensities of the inner and outer rings, the observer adjusted the luminance of the matching disk to achieve a brightness match to the test disk. The luminance of the ring surrounding the matching disk was fixed.

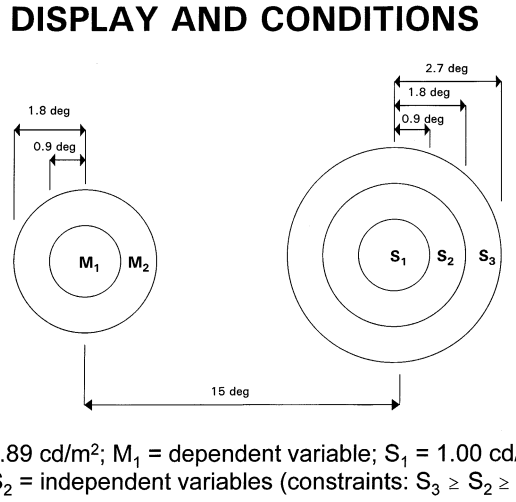

Fig. 2. Diagram of the visual stimulus used in the experiments. The luminance S_1 of the test disk was fixed at the value 1.00 cd m^{-2} throughout the study. The luminances S_2 and S_3 of the inner and outer test surrounds were manipulated as the independent variables over the range from 1.00 to 2.63 cd m^{-2} in equal steps of 0.17 log units and subject to the constraint that $S_3 \geq S_2$. The matching disk luminance M_1 was adjusted as the dependent variable to achieve a brightness match to the test. The luminance M_2 of the matching disk surround was fixed throughout the experiment at the value 5.89 cd m^{-2}.

Suppose that disk brightness is computed by a neural mechanism that performs *perfect* spatial edge integration and also instantiates the highest luminance anchoring rule. Perfect edge integration implies that the luminance ratios of spatially separated display regions will be computed as accurately as the luminance ratios of nearby regions. Thus, disk brightness should depend *only* on the ratio of the disk luminance to the highest luminance within that region's perceived frame of illumination. In our study this implies that disk brightness should depend only on the ratio of the disk luminance to that of the *outer* annulus.

On the other hand if there were no spatial edge integration whatsoever, disk brightness should depend only on the luminance ratio of the disk to its *immediate* surround, in other words its border contrast. Thus, in our experiment, disk brightness should depend only on the luminance of the *inner* annulus.

It will be shown that neither of these hypotheses can account for our data. More importantly, the data also rule out a compromise model that incorporates a distant-dependent weighted integration of local contrast. The inner and outer annuli work together in a considerably more complicated way to determine disk brightness. To account for our brightness matching results, we will present an alternative model of edge integration based on an underlying neural filling-in mechanism. In our model, a brightness signal is assumed to spread spatially from locations of edges in a retinotopic neural representation of the image. The model postulates that the strength of the spreading brightness signal is modulated by the luminance ratios of edges crossed along the path of spatial diffusion. It will be shown that this model provides a quantitative account of our data, including observed failures of brightness constancy.

2. Experiment

2.1. Visual display

The visual display consisted of two disks, surrounded by rings, as illustrated in Fig. 1 and diagrammed in Fig. 2 (see Section 2.3 for explanation of the *S* and *M* labels in Fig. 2). The radii of the test and matching disks were both 0.9°. The outer radii of the inner ring and match-

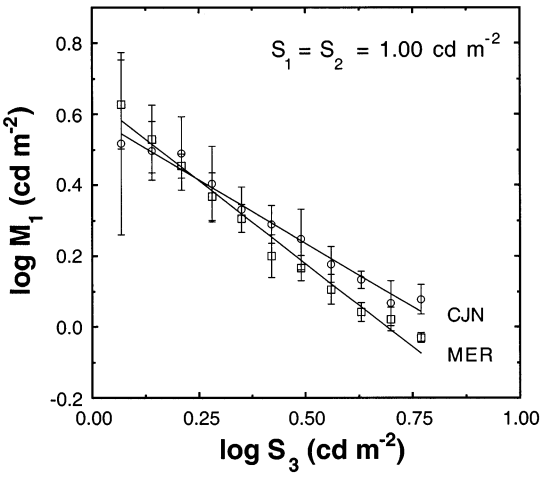

Fig. 3. Brightness matches as a function of outer ring luminance for the block of trials in which $S_2 = S_1 = 1.00$ cd m^{-2}. When $S_2 = S_1$, the test configuration appears as a disk surrounded by a single wide annulus, comprising inner and outer rings of equal luminance. For each subject, test brightness decreased as a power function of outer ring luminance. On this log–log plot, the power law function is a straight line. The power law exponent is given by the slope of the line (-0.9365 for subject MER and -0.7155 for subject CJN).

ing ring were both 1.8°. The outer radius of the outer ring was 2.7°.

The stimulus was viewed through a haploscope so that in later experiments (the results of which will be presented in future papers) the disks could be separated from their surround rings in apparent depth and the data could be compared with the data reported here. Identical stimuli, each having the spatial layout shown in Fig. 2, were generated simultaneously on dual computer monitors (Radius Model TX-D2151RD, 60 Hz refresh, 1280×1024) mounted in a mirror haploscope with two 40% reflective (60% transmissive) plate-glass type beam splitters measuring $127 \times 178 \times 3$ mm^3 (Edmund Scientific #61-260). Only the green guns of the monitors were used to produce the stimuli. The two mirrors of the haploscope were positioned at approximately a 45° angle with respect to the subject's line of sight. Both the accommodation (2.81 diopters) and the vergence angle were matched to the 35.5 cm viewing distance of the stimuli. Luminance values of the two monitors were linearized using lookup tables that specified the calibrated hardware value required to produce the desired luminance values. The luminances of the disks and rings were monitored periodically at the output end of each channel of the haploscope throughout the experiment with a Spectra Pritchard photometer (Photo Research, Model 1980A). Luminance values were restricted to a small range of low mesopic intensities (between 1 and 6 cd m^{-2}), which may restrict the applicability of our conclusions.

The display was controlled by custom software running on an Apple MacIntosh 9500 computer.

2.2. Observers

Two observers served as subjects. One of the observers (MER), a 45-year-old male, is the first author of this paper. MER was an experienced psychophysical observer and was aware of the experimental hypotheses. The second observer (CJN), a 33-year-old male, was a Psychology graduate student. CJN was also an experienced psychophysical observer, but he was naive with respect to the hypotheses. Neither observer was aware of the quantitative models of the data to be presented in the Section 2.4, because these models were developed only after all of the data had been collected.

2.3. Procedure

Each of the two observers viewed the display and adjusted the physical intensity M_1 of the disk on the left-hand side of the display (matching disk) through the use of a slider until it appeared equal in brightness to the disk on the right (test disk). The observers were instructed to alternative between the looking at the test and matching disks and to judge the appearance of each disk only when that disk was presented foveally.

Brightness matches were carried out at different values of inner and outer ring luminance, denoted S_2 and S_3, respectively. S_1 was fixed at 1.00 cd m^{-2} throughout the experiment. *Across blocks* of trials, S_2 was varied in logarithmic steps of 0.17 log units from $S_1 =$ 1.00 to 2.63 cd m^{-2}. *Within blocks*, S_2 was fixed and S_3 was varied in equal logarithmic steps of 0.17 log units, from S_2 to 2.63 cd m^{-2} (with the exception of the block corresponding to $S_2 = 1.00$ cd m^{-2}, in which S_2 was varied from 1.17 to 2.63 cd m^{-2} and, for MER only, the block corresponding to $S_2 = 1.17$ cd m^{-2}, in which S_3 was varied from 1.38 to 2.63 cd m^{-2}). The luminance M_2 of the matching disk surround was fixed at 5.89 cd m^{-2}. This luminance was always either equal to or greater than that of any other region within the display. The background was black.

The experiment was conducted in a small booth, surrounded by matte black drapes, housed in a dark room. The subjects dark-adapted for at least 3 min before each experimental session. A single block of trials took about 45–90 min to complete. Subjects typically ran only one or two blocks of trials in any given day, with a substantial rest period in between blocks whenever two blocks were run on the same day.

2.4. Results and analysis

Fig. 3 shows how the responses (i.e. luminance setting M_1 of the matching disk) of the two subjects varied as a function of S_3 for the particular block of trials in which $S_2 = S_1 = 1.00$ cd m^{-2}.

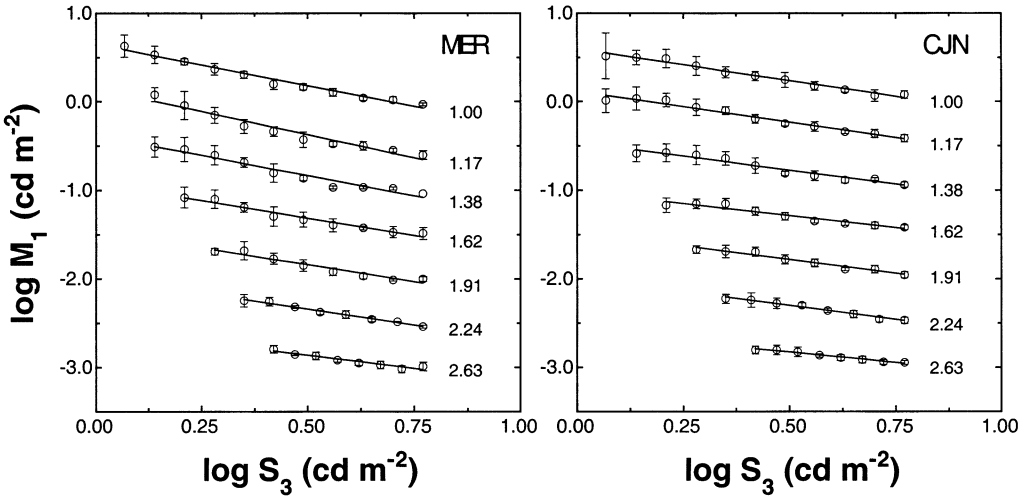

Fig. 4. Log M_1 as a function of log S_3 at the seven levels of S_2 tested in the experiment. At each level of S_2, log M_1 is a linearly-decreasing function of log S_3, implying that brightness matches are power functions of outer ring luminance. Power law exponents were estimated from the slopes of the best-fitting regression lines. The exponent of the power law relating M_1 to S_3 decrease with increasing inner ring luminance S_2. The separate data plots are labeled with the raw S_2 values (in units of cd m^{-2}). The plots have been shifted down by 0.5 log units on the y-axis for each successive value of S_2 for clarity.

Under these conditions, the test configuration appeared as a large disk with a single surround of luminance S_3, similar to Wallach's stimulus, except that, here, the disks on the two sides of the display were unequal in area. The data in Fig. 3 is plotted on a log-log scale, which reveals that log M_1 is related to log S_3 by the linear equation

$$\log M_1 = k_0 - k_1 \log S_3. \tag{1}$$

By taking the antilog of both sides of Eq. (1), we see that M_1 is related to S_3 by a *power law*:

$$M_1 = \frac{10^{k_0}}{S_3^{k_1}}. \tag{2}$$

When $k_1 = 1$, Eq. (2) is equivalent to Wallach's ratio rule. This is shown as follows. In this particular block of trials $S_2 = S_1 = 1.00$ cd m^{-2}, so the stimulus disk and inner annulus together formed one large disk of fixed luminance 1.00 cd m^{-2}. Call the luminance of this large disk $S_{1,2}$. Then, according to the ratio rule,

$$\frac{M_1}{M_2} = \frac{S_{1,2}}{S_3}. \tag{3}$$

M_2 and $S_{1,2}$ were both held constant in the experiment. Setting $M_2 S_{1,2} = 10^{k_0}$, and $k_1 = 1$ we recover Eq. (2).

For subject MER, $k_1 \simeq 1$ and the ratio rule holds. For subject CJN, $k_1 = 0.713$ and the ratio rule does *not* hold. Nevertheless, *both* observers' brightness matches are consistent with a *generalized ratio rule* of the form

$$\frac{M_1}{M_2} = \frac{S_{1,2}}{S_3^{k_1}}, \quad \text{where } k_1 \leq 1. \tag{4}$$

One possible explanation of CJN's failure to produce Wallach's ratio rule in this particular block of trials is the fact that the test and matching disks differed in size, whereas, in Wallach's experiment they were the same size. Thus, there is no strong theoretical reason for brightness constancy to hold.

In Fig. 4 are presented similar log–log plots of matching disk luminance vs outer ring luminance corresponding to seven different values of inner ring luminance. The inner ring luminances are equally spaced on a log scale. Each plot represents data collected in a separate block of trials.

For each subject, and for every level of S_2, log M_1 depended linearly on log S_3, as in Eq. (1), with the *intercept k_0 and slope k_1 being dependent in general on the value of S_2*. For each level of S_2, estimates of k_0 and k_1 were obtained by fitting linear regression equations to the plots of log M_1 vs log S_3. The best-fitting regression lines are plotted in Fig. 4 along with the data. The intercepts, slopes, and correlation coefficients for these regression analyses are presented in Table 1.

Table 1
Parameters derived from fitting the lightness matching data with a regression model of the form: $\log M_1 = k_0 - k_1 \log S_3$

MER							
S_2	1.00	1.17	1.38	1.62	1.91	2.24	2.63
k_0	0.647	0.650	0.622	0.582	0.542	0.521	0.436
k_1	0.936	1.048	0.915	0.792	0.764	0.723	0.602
r^2	0.980	0.953	0.958	0.962	0.945	0.990	0.929
CJN							
S_2	1.00	11.17	1.38	1.62	1.91	2.24	2.63
k_0	0.594	0.617	0.544	0.488	0.528	0.518	0.404
k_1	0.716	0.696	0.636	0.547	0.619	0.638	0.469
r^2	0.980	0.968	0.953	0.935	0.962	0.978	0.972

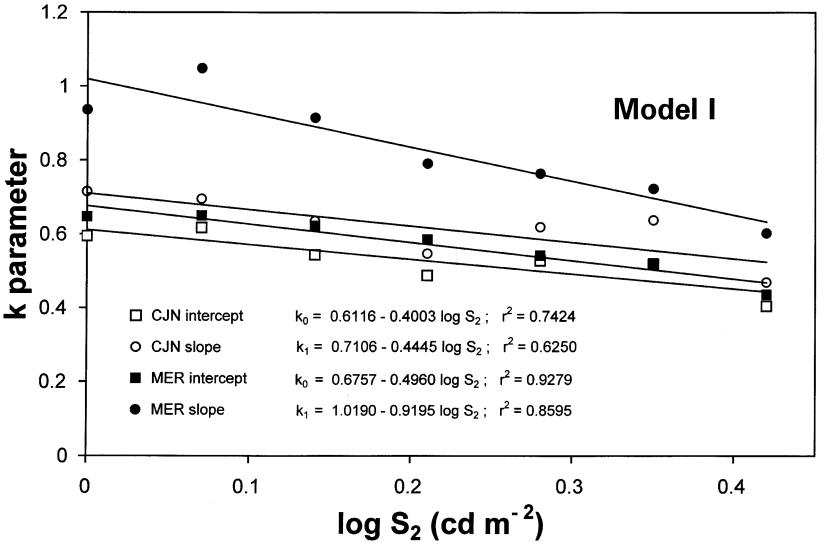

Fig. 5. Brightness matching equation Model I. The slopes k_1 and intercepts k_0 of the regression lines in Fig. 4 (each corresponding to an equation of the form: $\log M_1 = k_0 - k_1 \log S_3$) are plotted as a function of $\log S_2$. k_1 and k_0 have been modeled as linear functions of $\log S_2$ for each of the two subjects. The regression lines corresponding to the best-fitting linear models are plotted with the data. The corresponding regression equations are listed on the plot.

From inspection of Table 1, it can be seen that the estimates of k_0 and k_1 tend to decrease as the value of the inner ring luminance S_2 is increased. This implies that, *the higher the value of* S_2, *the less* S_3 *influences disk brightness*.

Fig. 5 illlustrates how the estimates of the slope k_0 and intercept k_1 of Eq. (1) depend on $\log S_2$. The plots are approximately linear. To characterize the S_2-dependence of the brightness matches, the k_0 estimates were therefore modeled with the linear equation

$$k_0 = \zeta_1 - \zeta_2 \log S_2, \tag{5}$$

and the S_2-dependence of the k_1 estimates were modeled with a similar linear equation:

$$k_1 = \zeta_3 - \zeta_4 \log S_2. \tag{6}$$

Substituting Eqs. (5) and (6) into Eq. (1) yields

$$\log M_1 = \zeta_1 - \zeta_2 \log S_2 - \zeta_3 \log S_3 + \zeta_4 \log S_2 \log S_3. \tag{7}$$

Eq. (7) provides a complete quantitative model of our brightness matching data. We hereafter refer to it as the *brightness matching equation*.

Negative terms on the right side of the matching equation represent *darkness induction* effects and *positive* terms represent *brightness induction* effects. The magnitude of each effect is given by the value of the ζ (the Greek letter Zeta) coefficient associated with that effect.

A hierarchical regression procedure was used to fit the data with Eq. (1), then Eqs. (5) and (6). From this procedure the following sets of ζ coefficients were obtained for each of the two subjects. CJN: $\zeta_1 = 0.6116$; $\zeta_2 = 0.4003$; $\zeta_3 = 0.7106$; $\zeta_4 = 0.4445$. MER: $\zeta_1 = 0.6757$; $\zeta_2 = 0.4960$; $\zeta_3 = 1.0190$; $\zeta_4 = 0.9195$. The correlation coefficients associated with the linear model of k_0 were 0.8616 (CJN) and 0.9633 (MER). The correlation coefficients associated with linear model of k_1 were 0.7906 (CJN) and 0.9271 (MER).

This four-parameter statistical model of our brightness matching data will hereafter be referred to as Model I, to distinguish it from a slightly more complex—but theoretically motivated—five-parameter model of the data (Model II) to be derived in the next section. To help motivate Model II, we next consider possible mechanistic interpretations of Eq. (7).

2.5. Luminance gain control account

Any induction effect that is *subtractive* (*darkness* induction) when brightness matching is described in terms of log luminances can be described as a *divisive* inhibition, or gain control, when matching is described in terms of raw luminance values. This point is illustrated by our earlier derivation of Eq. (2) from Eq. (1). It follows that the second and third terms on the right-hand side of Eq. (7) can be thought of as separate and independent gain controls exerted by S_2 and S_3 on S_1 to control disk brightness. In other words, S_2 or S_3 each operates on the disk by *dividing* the disk luminance by a magnitude that is a power of S_2 or S_3 to modulate disk brightness. The coefficients ζ_2 and ζ_3 specify the power law exponents (as in Eq. (4)) of the gain control exerted on the disk by S_2 and S_3, respectively.

For subject MER, the outer ring exerted a *Weber's law* gain control (i.e. power law exponent for $S_3 = \zeta_3 \simeq$

1). For subject CJN, the gain control was somewhat weaker ($\zeta_3 \simeq 0.71$). For both subjects, the inner ring exerted an additional, but weaker, gain control with a power law exponent equal to about 0.43 for CJN and 0.50 for MER. This analysis suggests an interpretation of the data in terms of a *strong nonlocal gain control* exerted by the region of highest luminance and a *weaker local gain control* exerted by the immediately adjacent region.

In addition to these independent S_2- and S_3-derived gain controls, there was an additional tendency for S_2 to interact with S_3 in the log domain to produce some *brightness* induction as opposed to darkness induction, as indicated by the *positive* term involving $\log S_2 \log S_3$ on the right-hand side of Eq. (7). The strength of the brightness induction due to the $\log S_2 \times \log S_3$ interaction is given by the parameter ζ_4, which is 0.44 for CJN and 0.92 for MER. This brightness induction effect does *not* have a natural interpretation in terms of a gain control because it cannot be expressed as a simple divisive inhibition when the logarithmic equation is transformed into an equation involving raw luminances.

Alternate ways of writing Eq. (7) suggest alternative interpretations of the $\log S_2 \times \log S_3$ interaction. Rewriting Eq. (7) in the form

$$\log M_1 = \zeta_1 - (\zeta_2 - \zeta_4 \log S_3)\log S_2 - \zeta_3 \log S_3, \quad (8)$$

suggests that the power law exponent of the gain control due to S_2 is a function of S_3. One way that this could come about would be for S_3 to inhibit S_2, and thus indirectly to *disinhibit* S_1.

Alternatively, rewriting Eq. (7) in the form,

$$\log M_1 = \zeta_1 - \zeta_2 \log S_2 - (\zeta_3 - \zeta_4 \log S_2)\log S_3, \quad (9)$$

suggests that the power law exponent of the gain control due to S_3 is a function of S_2. In this interpretation, the darkness induction exerted by the highest luminance weakens as S_2 increases. In the next section, we derive a mechanistic account of the data that is consistent with the latter interpretation of the data, although the theory that we will offer will be expressed in terms of neural filling-in processes, rather than in terms of gain control operations.

3. Filling-in model

Eq. (9) suggests that somehow the luminance S_2 of the inner annulus is modulating the influence of S_3. We next derive a model that accounts for this modulation in terms of a darkness filling-in mechanism. The model shares many properties with both the Retinex theory of Land and McCann (1971), Land (1977), Land (1986) and the BCS/FCS brightness filling-in model of Grossberg and colleagues (Cohen & Grossberg, 1984; Grossberg & Mingolla, 1985a,b, 1987; Grossberg & Todorović, 1988). However, the new model also differs from both Retinex and the BCS/FCS model in significant ways. The similarities and differences between these models will be addressed in Section 6.1.

The model consists of five postulates. Postulates i–iv describe the presumed neurophysiological mechanisms underlying darkness induction. Postulates v and vi are more ad hoc and unlike Postulates i–iv, they apply only to the double-ring experiment. They are, nevertheless, required for self-consistency. An attempt to ground the ad hoc postulates in terms of more fundamental mechanistic assumptions is made in Section 6.6.

4. Model postulates

i. There exist neural signals derived from local luminance borders in the image that have magnitude proportional to the log of the luminance ratio I_{max}/I_{min} across the border, where I_{max} is the luminance of the region on the most luminant side of the border and I_{min} is the luminance of the region on the least luminant side of the border. These signals will be referred to as *border signals*.

ii. Border signals act as sources of *achromatic color signals* that have magnitudes proportional to the log luminance ratios of their source borders and spread isotropically over time from the locations of the source borders within a neural representation, or map, of the visual image.

iii. When a color signal tries to diffuse across the location of a border signal in the neural map, a percentage of a color signal is blocked.

iv. The percentage of a color signal that is blocked by a border signal is proportional to the log luminance ratio of the border associated with the border signal that does the blocking.

v. In the double-ring experiment, the effects on brightness matching (if any) of the border between the matching ring and the background, and of the border between the outer test ring and the background, are negligible.

vi. In the double-ring experiment, any effects of the matching disk and matching ring luminances on test disk brightness are negligible.

5. Quantitative model of brightness matching

Raising the luminance of either the inner or outer annulus tends to *darken* the test disk. We therefore assume that the achromatic color signal that flows into the interior region of cortical representation of the test

disk signals darkness, rather than brightness. According to the postulates of the model, this signal has the form

$$-\Delta B_{\text{test}} = \beta_1 \log\left(\frac{S_2}{S_1}\right) + (1-\gamma)\,\beta_2 \log\left(\frac{S_3}{S_2}\right), \tag{10}$$

where the negative sign in front of the quantity ΔB_{test} is included as a reminder that darkness induction represents a *negative* change in test disk brightness. This negative 'change' is presumably relative to some internally generated brightness signal: the so-called 'dark light' or *eigengrau* (Müller, 1896).

The two additive terms on the right side of Eq. (10) represent the darkness induction signals diffused into the disk interior from the S_2/S_1 and S_3/S_2 borders, respectively. Each term is proportional to the log luminance ratio of the border that acts as its source. The quantity γ is the percentage of the signal generated by the S_3/S_2 that is stopped by the S_2/S_1 border. It follows that the quantity $(1-\gamma)$ is the percentage that is *not* stopped and therefore passes through the S_2/S_1 border to darken the disk. The parameters β_1 and β_2 are free parameters that might depend on the spatial separation of borders. For example, the signal generated at the S_3/S_2 border might be expected to have a weaker effect on disk brightness than the signal generated at the S_2/S_1 border because the S_3/S_2 border is further from the disk, even if there were no blockage of the S_3/S_2 signal by the S_2/S_1 border.

According to Postulate iv, the percentage of the flow that is blocked by a border is directly proportional to the log luminance ratio of the border doing the blocking, which in this case is $\log S_2/S_1$. Denoting the constant of proportionality by α, we rewrite Eq. (10) in the form

$$-\Delta B_{\text{disk}} = \beta_1 \log\left(\frac{S_2}{S_1}\right) + \left(1-\alpha\log\left(\frac{S_2}{S_1}\right)\right)\beta_2 \log\left(\frac{S_3}{S_2}\right). \tag{11}$$

To derive a theoretical brightness matching equation for the double-ring experiment, we must also compute the darkness induction signal exerted on the matching disk by its surround. Postulates v and vi allow us to ignore effects of the outer border of the matching annulus, as well as any potential effects of the test configuration. The darkness induction signal for the matching disk therefore has the form

$$-\Delta B_{\text{match}} = \beta_1 \log\left(\frac{M_2}{M_1}\right) = \beta_1 \log M_2 - \beta_1 \log M_1. \tag{12}$$

A brightness match between the stimulus and matching disks will be achieved if and only if the magnitudes of the darkness induction are equal in the two cases, such that $-\Delta B_{\text{test}} = -\Delta B_{\text{match}}$. To achieve a brightness match, we therefore set Eq. (11) equal to Eq. (12) to obtain

$$\beta_1 \log M_2 - \beta_1 \log M_1 = \beta_1 \log\left(\frac{S_2}{S_1}\right) + \left(1-\alpha\log\left(\frac{S_2}{S_1}\right)\right)\beta_2 \log\left(\frac{S_3}{S_2}\right). \tag{13}$$

In our experiment, $\log M_2 = 0.77$ and $\log S_1 = 0$. Making these substitutions in Eq. (13) and rearranging terms, we obtain the following theoretical brightness matching equation:

$$\log M_1 = 0.77 - \left(1-\frac{\beta_2}{\beta_1}\right)\log S_2 - \left(\frac{\alpha\beta_2}{\beta_1}\right)\log^2 S_2 - \left(\frac{\beta_2}{\beta_1}\right)\log S_3 + \left(\frac{\alpha\beta_2}{\beta_1}\right)\log S_2 \log S_3. \tag{14}$$

5.1. Re-analysis of the data based on the darkness filling-in model

The theoretical brightness matching equation derived from the filling-in model (Eq. (14)) has the same form as the statistical brightness matching equation that we used to fit the data (Eq. (7)) *except* for the fact that it includes an extra term that is quadratic in $\log S_2$ (i.e. depends on $\log^2 S_2$). In our original data analysis, we did not consider the possibility of fitting the data with a term that was quadratic in $\log S_2$ because we had no a priori reason to expect such a term. To allow for the quadratic term, Eq. (5) (which models the intercept of Eq. (1)) is replaced by

$$k_0 = \xi_1 - \xi_2 \log S_2 - \xi_3 \log S_2, \tag{15}$$

and Eq. (6) (which models the slope of Eq. (1)) is replaced with

$$k_1 = \xi_4 - \xi_5 \log S_2. \tag{16}$$

This results in a new linear regression model of the brightness matching data (Model II):

$$\log M_1 = \xi_1 - \xi_2 \log S_2 - \xi_3 \log^2 S_2 - \xi_4 \log S_3 + \xi_5 \log S_2 \log S_3. \tag{17}$$

The data was reanalyzed on the basis of Model II, using Eq. (15) to model k_0 and Eq. (16) to model k_1 (see Fig. 6), and the following sets of ξ (Greek letter Xi) coefficients were obtained for each of the two subjects. CJN: $\xi_1 = 0.6013$; $\xi_2 = 0.2240$; $\xi_3 = 0.4197$; $\xi_4 = 0.7106$; $\xi_5 = 0.4445$. MER: $\xi_1 = 0.6517$; $\xi_2 = 0.0849$; $\xi_3 = 0.9788$; $\xi_4 = 1.0190$; $\xi_5 = 0.9195$.

For both subjects, making the switch from Model I (intercept k_0 linear in $\log S_2$) to Model II (k_0 quadratic in $\log S_2$) produced a small improvement in the correlation coefficients associated with the regression analysis: 0.8459 $\Rightarrow$ 0.8686 (CJN) and 0.9633 $\Rightarrow$ 0.9905 (MER). But adding the quadratic term adds an extra degree of freedom to the model, so the plausibility of the theoretical model does not rest so much on the goodness of the statistical fit as on the issue of whether it is possible to

give a sensible and self-consistent interpretation of the estimated values of the ξ coefficients in terms of the underlying parameters β_1, β_2, and α of the filling-in model.

Comparison of Eq. (14) and Eq. (17) suggests the identifications $\xi_1 = 0.77$; $\xi_2 = 1 - \beta_2/\beta_1$; $\xi_3 = \xi_5 = \alpha\beta_2/\beta_1$; and $\xi_4 = \beta_2/\beta_1$. From these identifications, we derived the following theoretical predictions, which were tested by examining the statistical estimates of the ξ coefficients.

Prediction 1: $\xi_3 = \xi_5$. The percent error in this prediction is $2(\xi_3 - \xi_5)/(\xi_3 + \xi_5)$. The errors for the two subjects are -5.74% (CJN) and $+6.25\%$ (MER). The fact that the errors for the two subjects are both small and in opposite directions suggests that the errors are measurement errors.

Prediction 2: $\xi_4 = 1 - \xi_2$. The percent error in this prediction is the difference in the values on the two sides of the equation divided by the average value: $2(\xi_4 + \xi_2 - 1)/(\xi_4 - \xi_2 + 1)$. The percent errors for the two subjects are -8.80% (CJN) and $+10.74\%$ (MER). Again, the fact that the errors are in opposite directions suggests that the errors are measurement errors.

Prediction 3: $\xi_1 = 0.77$. The percent error in this prediction is $(\xi_1 - 0.77)/0.77$. For the two subjects, the percent errors are -21.9% (CJN) and -15.4% (MER). Since these errors are of moderate magnitude and in the same direction, they may represent a true discrepancy between the theory and the data. A likely source of the error is that we have neglected the potential effect of the outer border of the matching ring on the brightness of the matching disk in our model. At the same time, there is no a priori reason to expect that the statistical estimates of ξ_1 would be this close to the predicted value unless the model has some validity.

We performed the following additional analyses to test whether the estimated parameters can be sensibly interpreted in terms of an underlying filling-in process. According to the theory, ξ_4 and $1 - \xi_2$ should both be equal to β_2/β_1. The ratio β_2/β_1 can be estimated by averaging the statistical estimates of ξ_4 and $1 - \xi_2$, which yields the values 0.7433 (CJN) and 0.9671 (MER).

The parameter β_1 is naturally interpreted as the magnitude of the darkness induction signal that originates at the S_2/S_1 border and flows into the interior of the disk representation in the neural network. Similarly, β_2 is naturally interpreted as the magnitude of the darkness induction signal originating at the S_3/S_2 border that *would* flow into the interior of the disk representation *in the absence of any resistance to the signal at the* S_2/S_1 *border* (i.e. if the S_2/S_1 border were removed). The fact that the estimates of the β_2/β_1 ratio for the two subjects are both less than 1.0 can be interpreted as indicating that more of the S_3/S_2 signal would be lost en route to the disk interior during the process of diffusion than would be the S_2/S_1 signal in the absence of blockage of the S_3/S_2 signal by the S_2/S_1 border. This result makes sense in terms of the filling-in theory, because the S_3/S_2 signal must diffuse over a further distance than the S_2/S_1 signal to reach the disk interior.

The idea that border induction effects decrease with distance is consistent with the data of Reid and Shapley (1988) who demonstrated with a display that was similar, but not identical, to ours that the induction produced by circular contrast edge, surrounding but some

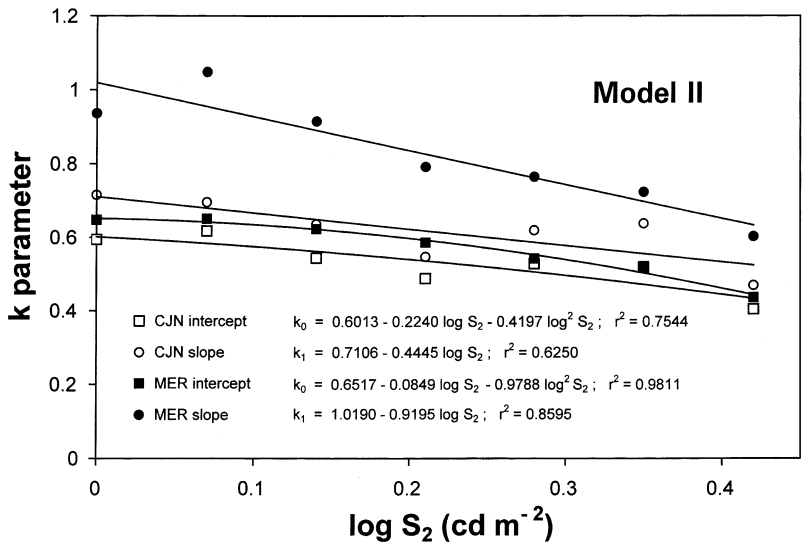

Fig. 6. Brightness matching equation Model II. The slopes k_1 and intercepts k_0 of the regression lines in Fig. 4 (each corresponding to an equation of the form: $\log M_1 = k_0 - k_1 \log S_3$) are plotted as a function of $\log S_2$ (as in Fig. 5). Here, k_1 has been modeled as a quadratic function of $\log S_2$. The regression lines corresponding to the best-fitting quadratic model of k_1 and linear model of k_0 for each subject are plotted with the data. The corresponding regression equations are listed on the plot.

distance away from the test disk perimeter, decreases as a function of distance. The relationship between our work and the work of Reid and Shapley is discussed further in Section 6.2.

As a final test of the model, the estimates of ξ_3 and ξ_5 obtained from the regression analysis were averaged to estimate the underlying theoretical quantity $\alpha\beta_2/\beta_1$. The resulting estimates were 0.4321 (CJN) and 0.9492 (MER). These estimates were then divided by the estimates of the ratio β_2/β_1 to obtain estimates of the theoretical parameter α for each of the two subjects. This yielded the values 0.5813 (CJN) and 0.9815 (MER).

The parameter α represents the constant of proportionality that relates the percentage of the S_3/S_2 signal blocked by the S_2/S_1 border to the value of $\log S_2/S_1$. The estimates of α differ for the two subjects. Nevertheless, when these estimates of α are multiplied by the values of $\log S_2/S_1$ that were used in the study, they produce percentages of blocked signal in the 0–1 range, as is required for a sensible mechanistic interpretation of the parameters. In fact, without exception, the results of our quantitative analyses lead to a sensible interpretation in terms of an underlying neural filling-in process.

6. Discussion

6.1. Relationship of our model to the BCS/FCS model and Retinex theory

We have shown that it is possible to give a quantitative account of our darkness induction data on the basis of a model of a neural filling-in process in which spreading darkness signals are partially blocked when they cross luminance edge boundaries. Our filling-in model borrows from both Retinex theory (Land & McCann, 1971; Land, 1977, 1986) and the BCS/FCS filling-in model (Cohen & Grossberg, 1984; Grossberg & Mingolla, 1985a,b, 1987; Grossberg & Todorović, 1988) the idea that brightness is computed by a neural process involving spatially-spreading signals that originate from luminance edges. In common with Retinex, but not with the BCS/FCS model, our model assumes that the magnitudes of the spreading signals are proportional to the log luminance ratios of the edges from which they are derived. In common with the BCS/FCS model, but not with the Retinex, our model assumes that the flow of the brightness signal (or, in this case, *darkness* signal) is resisted, or gated, at encountered borders.

Our model departs from the BCS/FCS model by assuming that the strength of this resistance is proportional to the log luminance ratio of the border doing the gating. The equations of the BCS/FCS model allow for a modulation of gating strength, but the mathematical form of this modulation is *not* equivalent to the log luminance ratio-dependent gating strength assumed in our model. In the BCS/FCS model, the gating of filling-in signals at borders is achieved by a shunting inhibition mechanism that *divides* the propagating signal by the contrast of the gating border. Our data indicate that a *percentage* of the propagating signal is blocked and this implies an underlying *multiplicative*, rather than a divisive, mechanism. The quantitative predictions of the two models are thus testably distinct and the BCS/FCS model can be ruled out as an alternative explanation of our data.

The BCS/FCS model also does not explicitly address the need for a darkness filling-in mechanism, as distinct from a brightness filling-in mechanism (Arrington, 1996). But a darkness filling-in mechanism is clearly required to account for our data on darkness induction.

In other ways, the assumptions of our model are consistent with those of the BCS/FCS model. In particular, our model is consistent with the key tenets of the BCS/FCS model that: (1) perceptual borders are synthesized by the visual nervous system from information about luminance edges; and (2) the colors of regions lying between or within borders are filled-in on the basis of spreading neural activity originating at the locations of luminance edges within a topographic neural map of the visual world. Our experimental results are part of a growing body of psychophysical and neurophysiological evidence (Arrington, 1994; Paradiso & Nakayama, 1991; Paradiso & Hahn, 1996; Rossi & Paradiso, 1996; Rossi, Rittenhouse, & Paradiso, 1996) that supports these assumptions.

Our model can be alternatively viewed as a modified Retinex model in which edge integration is weakened by intervening edges. This assumption has no precedence in Retinex theory, as originally presented or in other previously proposed Retinex-like models. In fact, it is at odds with the expressed goal of Retinex, which is to reconstruct the pattern of relative reflectances in the retinal image by perfectly integrating luminance ratios across space. The brightness values that Retinex assigns to surfaces or patches within the image have the same ratio relations to one another that the actual surface reflectances do. Our model does not share this property with Retinex. In our model the ratios of the brightness values assigned to nonadjacent regions of the retinal image will generally be *less than* the true reflectance ratios of these regions as a result of the border blockage of flowing color signals. Furthermore, these brightness ratios will progressively deviate from the true reflectance ratios as the number of edges lying along the path between the regions is increased. Thus, unlike Retinex, our model does not obey the principle of brightness constancy.

6.2. Relationship of our model to the work Reid and Shapley

Reid and Shapley (1988) (see also Shapley & Reid (1985)) proposed a different modification of Retinex theory in which edge integration declines as a function of edge separation. Their idea is fundamentally different from our blockage idea. We propose that edge integration weakens as a function of the *number* and *log luminance ratios* of borders encountered along the path between the edges whose influences are being integrated. Nevertheless, our blockage hypothesis does not rule out the possibility that there is also a falloff in edge integration due to spatial separation. One of us (Rudd, in preparation) has performed additional experiments with our two-annulus display, in which edge separation was varied while the number of intervening edges was held fixed. This procedure holds blockage constant while varying edge separation. The results of these experiments indicate that there *is* an independent effect of edge separation over and above the effect of contrast-dependent blocking. But blockage must also be assumed in order to account for our brightness matching data; distance-dependent modulation of the strength of edge integration is not enough.

6.3. Relationship to spatial filtering models

Because induction strength does not depend only on distance alone, but also, critically, on the number and log luminance ratios of intervening edges, our results cannot be accounted for by a mechanism based on a simple spatial weighting of luminance or edge signals. Even if it was assumed that raw luminance or contrast signals were converted to log units prior to spatial weighting, a linear weighting mechanism would not be able to account for the nonlinear ($\log^2 S_2$ and interaction) terms on the right-hand side of Eq. (17) (the brightness matching equation).

6.4. Brightness versus lightness

The word 'brightness' has been throughout this paper to refer to the subjective intensities of both real surfaces, as in Wallach's study, and the luminous regions of CRT displays. In the context of a study using Mondrian patterns as stimuli, Arend & Goldstein (1987) argued that CRT displays can be viewed as 'simulated surfaces'. They demonstrated that observers are able to judge either the perceived reflectance of these simulated surfaces—a quantity that they called 'lightness'—or their perceived luminances, which the authors referred to as 'brightness.' In general, these two types of judgments behave differently (Arend & GoldsteinArend & Spehar, 1993a,b; Schirillo, 1999a,b; Schirillo & Shevell, 1993; Schirillo, Reeves, & Arend, 1990).

It is unclear whether simple disk-and-ring displays of type used in the current study can produce differently-behaving lightness and brightness percepts. In our experiments, subjects were simply instructed to judge the subjective intensity of the disks. Because these instructions might be expected to elicit brightness judgments (as defined by Arend & Goldstein, 1987) and because the word 'brightness' is often used in the older literature to signify *any* type of stimulus intensity judgment, we refer here to the percepts studied in our experiment as 'brightness'.

The possible relevance our model to *lightness* perception remains to be demonstrated, but we suspect that the model will also help to explain some aspects of lightness. A connection between lightness and brightness is to be expected to the extent that both types of percepts depend on some of the same underlying early neural mechanisms and it seems at least plausible that filling-in is such a mechanism.

6.5. Equivalent backgrounds

An issue of some controversy within the field of brightness/lightness research is the question of whether one can always find a uniform surround that produces an induction effect of the same magnitude as an inhomogeneous surround. In a study by Bruno et al. (1997), observers compared a stimulus comprising a test surface surrounded by two, three, or four surfaces, each having a different luminance (inhomogeneous surround), to a comparison surface surrounded by a uniform field. Matches between the test and comparison surfaces were achieved when the luminance of the uniform surround was close to the *highest* luminance within the inhomogeneous surround. Models based on either space-averaged luminance or spaced-average contrast of the inhomogeneous surround produced poorer fits to the data.

In another study comparing the effects of homogeneous and inhomogeneous surrounds, however, Schirillo and Shevell (1996) found that the effect of inhomogeneous checkerboard surrounds on *increments* was not equivalent to that of a homogeneous surround of *any* luminance; whereas, with decrements, an inhomogeneous surround had about the same effect as the *space-averaged* luminance of an inhomogeneous surround. This result appears to be in conflict with results of the study by Bruno et al. (1997).

Our data is not consistent with *either* the idea that induction depends only on the highest luminance within the surround or with the idea that induction depends on the space-averaged surround luminance. The presence of an interaction term in the brightness matching equation (Eq. (17)) indicates that the inner and outer annulus instead modulate each other's induction effects in a more complex way.

6.6. Test/comparison isolation and directional filling-in

The model presented here quantitatively accounts for the results of the double-ring experiment, despite the fact that we have explicitly modeled the induction effects of only three of the five borders in the display. The induction effects that the model explicitly accounts for are the ones generated by the border between the test disk and the inner ring, the border between the inner and outer rings, and the border between the matching disk and its surround. These three borders are all dark-inside/light-outside, and thus would be expected to induce darkness in the disks. We have not modeled the effects of either the outer border of the matching ring or the outer border of the outer test ring. These borders are light-inside/dark-outside and thus would to induce brightness in the disks.

The fact that the model works despite the fact that it only takes in to account a subset of the borders justifies Postulates v and vi, which state that the borders between the background and the stimulus and matching configurations have a negligible effect on brightness matching (Postulate v), and that the matching configuration has a negligible effect on test disk brightness (Postulate vi).

A more comprehensive model of achromatic color induction would presumably specify how darkness and brightness filling-in signals each contribute to the percept of the double-ring display and to achromatic order, more generally. Such a model would need to explain why brightness induction signals had a negligible effect on brightness matching in our experiment.

The Directional Filling-In (DFI) model, previously proposed by one of the authors (Arrington, 1996), specifies one method by which complementary brightness and darkness filling-in signals are generated, propagate, and combine. The DFI model assumes that separate brightness and darkness induction signals spread within independent filling-in networks and are subsequently summed to produce an achromatic color signal. Within each network, spreading filling-in signals are differentially gated by encountered edges, depending on edge contrast polarity. According to the DFI model, brightness signals flow unimpeded across borders in the dark-to-light direction and are totally blocked by borders in the light-to-dark direction. Darkness signals behave in a symmetrical way: they flow unimpeded across borders in the light-to-dark direction and are totally blocked by borders in the dark-to-light direction.

The results of our double-ring experiment force the conclusion that the DFI model's assumption of unimpeded flow of the darkness signal in the light-to-dark direction must be replaced by the alternative assumption that a proportion of the signal flowing in this direction is in fact blocked. And, this proportion is directly related to the log luminance ratio of the blocking border. A more detailed analysis of how a neural filling-in model that includes separate lightness and darkness induction networks and appropriate blockage could account for the phenomenology of the double-ring display as a whole can be found in a recent paper by Rudd (2001).

6.7. Image segmentation, frameworks, and articulation

We conclude the paper with some speculative comments about how such a filling-in model might be further elaborated to account for some aspects of brightness and lightness perception that appear to depend on figural organization or on unconscious inferences about the nature of the illumination.

It seems likely that the magnitude of edge blocking is modulated by image segmentation cues. For example, luminance regions that appear to be in different depth planes might be expected to exert weaker induction effects on one another than do regions lying in the same depth plane (although the experiment evidence on this is equivocal; see Wolff, 1933; Gibbs & Lawson, 1974; Schirillo & Shevell, 1993; Gilchrist et al., 1999). If so, the effect could potentially be accounted for by a model in which blocking strength depends on whether the regions on either side of the border appear to lie at the same depth. Blocking strength might thus be expected to be modulated by the presence in the image of border junctions—such as X-, Y-, T-, and ψ-junctions—that are believed by many researchers to control the image segmentation process (Adelson, 1993; Anderson, 1997; Todorović, 1997; Melfi & Schirillo, 2000). The rules of image segmentation are far from completely worked out and it might not be a trivial task to extend the model in this direction, but we think that it is a useful avenue to explore.

At the same time, it should be kept in mind that some brightness/lightness phenomena that are generally believed to depend on such 'high-level' segmentation mechanisms may be accounted for by the unelaborated filling-in presented in this paper. Consider research on frameworks of illumination, which is a topic of active research in the lightness literature (Gilchrist et al., 1999; see also Katz, 1935; Koffka, 1935). Theories of lightness perception that invoke the concept of frameworks assume that the visual system somehow figures out which groups of surfaces are being illuminated by a shared light source—these surfaces constitute a framework—and uses this knowledge in assigning lightness values to surfaces.

One visual cue that is believed to cause the surfaces within a framework to perceptually cohere is the degree of 'articulation', or number of different surfaces, in the framework (Burzlaff, 1931; Gilchrist et al., 1999). Schirillo (1999a,b) asked his subjects perform both

brightness (Schirillo, 1999a) and lightness (Schirillo, 1999b) matching tasks in which test and comparison patches were embedded in separate frameworks, each consisting of a surround containing a varying number of articulation patches (patches of either higher or lower luminance than the space-averaged surround luminance, with the constraint that the surrounds always had the same average luminance). The subjects' brightness and lightness judgments were more likely to exhibit constancy (i.e. conform to a local ratio rule based on the framework, as opposed to a global ratio rule based on the display as a whole) when the test was embedded in a framework consisting of a Mondrian comprising many patches than when the surround was less articulated.

Although this result appears superficially to require an explanation in terms of frameworks of illumination, the filling-in model proposed here can at least partially account for it. According to the model, articulation should favor a local brightness/lightness computation over global computation because articulation serves to isolate the test from the influence of the comparison patch and its immediate surround by introducing more edges and consequently more blocking of remote induction signals.

These ideas are admittedly speculative. We offer them here mainly to indicate how the darkness induction model that we have proposed could ultimately serve as a building block in a more elaborate neural theory of brightness and lightness perception.

Acknowledgements

The double-ring experiment was carried out at the AFRL Laboratory/Human Effectiveness Directorate, Mesa, AZ. Funds for the project were provided by a National Research Council Research Associate Award to the first author. The authors would like to thank Dr Richard A. Thurman and Dr Byron Pierce, the AFRL research advisors for the project, for providing accommodations and technical support, and Bill Morgan for programming and calibrating the experimental apparatus. Thanks also to an anonymous reviewer whose challenging criticisms greatly improved the quality of the paper.

References

Adelson, E. H. (1993). Perceptual organization and the judgment of brightness. *Science*, *262*, 2042–2044.

Anderson, B. (1997). A theory of illusory lightness and transparency in monocular and binocular images: the role of contour junctions. *Perception*, *26*, 419–453.

Arend, L. (1985). Spatial gradient illusions and inconsistent integrals. *Investigative Ophthalmology and Visual Science*, *26*(Suppl.), 280.

Arend, L. (1994). Surface colors, illumination, and surface geometry: intrinsic-image models of human color perception. In A. L. Gilchrist, *Lightness*, *brightness*, *and transparency* (pp. 159–213). Hillsdale, NJ: Erlbaum.

Arend, L., & Goldstein, R. (1987). Lightness models, gradient illusions, and curl. *Perception and Psychophysics*, *42*, 65–80.

Arend, L., & Spehar, B. (1993a). Lightness, brightness and brightness contrast: I. Illumination variation. *Perception and Psychophysics*, *54*, 446–456.

Arend, L., & Spehar, B. (1993b). Lightness, brightness and brightness contrast: II. Reflectance variation. *Perception and Psychophysics*, *54*, 457–468.

Arrington, K. F. (1994). The temporal dynamics of brightness filling-in. *Vision Research*, *34*, 3371–3387.

Arrington, K. F. (1996). Directional filling-in. *Neural Computation*, *8*, 300–318.

Blake, A. (1985). Boundary conditions for lightness computation in Mondrian world. *Computer Vision*, *Graphics and Image Processing*, *32*, 314–327.

Brown, R. O., & MacLeod, D. I. A. (1991). Induction and constancy for color saturation and achromatic contrast variance. *Investigative Ophthalmology and Visual Science*, *30*(Suppl.), 130.

Brown, R. O., & MacLeod, D. I. A. (1997). Color appearance depends on the variance of surround colors. *Current Biology*, *7*, 844–849.

Bruno, N. (1992). Lightness, equivalent backgrounds and the spatial integration of luminance. *Perception (Suppl.)*, 80.

Bruno, N., Bernardis, P., & Schirillo, J. A. (1997). Lightness, equivalent backgrounds, and anchoring. *Perception and Psychophysics*, *59*, 643–654.

Burzlaff, W. (1931). Methodologishe beiträge zum problem der farbenkonstanz. *Zeitschrift für Psychologie*, *119*, 117–235.

Cataliotti, J., & Gilchrist, A. L. (1995). Local and global processes in lightness perception. *Perception and Psychophysics*, *57*, 125–135.

Cohen, M. A., & Grossberg, S. (1984). Neural dynamics of brightness perception: features, boundaries, diffusion, and resonance. *Perception and Psychophysics*, *36*, 428–456.

Gelb, A. (1929). Die 'Farbenkonstanz' der Sehdinge [Colour constancy of visual objects]. In W.A. von Bethe, *Handbuch der normalen und pathologischen Physiologie* (Vol. 12, pp. 594–678). Berlin: Springer.

Gibbs, T., & Lawson, R. B. (1974). Simultaneous brightness contrast in stereoscopic space. *Vision Research*, *14*, 983–987.

Gilchrist, A. [L.], Delman, S., & Jacobsen, A. (1983). The classification and integration of edges as critical to the perception of reflectance and illumination. *Perception and Psychophysics*, *33*, 425–436.

Gilchrist, A. [L.], Kossyfidis, C., Bonato, F., Agnostini, T., Cataliotti, J., Li, X., & Spehar, B. (1999). An anchoring theory of lightness perception. *Psychological Review*, *106*, 795–834.

Grossberg, S., & Mingolla, E. (1985a). Neural dynamics of form perception: boundary completion, illusory figures, and neon color spreading. *Psychological Review*, *92*, 173–211.

Grossberg, S., & Mingolla, E. (1985b). Neural dynamics of perceptual grouping: Textures, boundaries, and emergent segmentations. *Perception and Psychophysics*, *38*, 141–171.

Grossberg, S., & Mingolla, E. (1987). Neural dynamics of surface perception: boundary webs, illuminants, and shape-from-shading. *Computer Vision*, *Graphics and Image Processing*, *37*, 116–165.

Grossberg, S., & Todorović, D. (1988). A neural network architecture or preattentive vision. *IEEE Transactions on Biomedical Engineering*, *36*, 65–84.

Helmholtz, H. von (1910/1925). *Helmholtz's treatise on physiological optics*, *volume III*. English translation by J. P. C. Southall from the 3rd German edition of Handbuch der physiologischen Optik. Menasha, WI: Optical Society of America.

Helson, H. (1943). Some factors and implications of color constancy. *Journal of the Optical Society of America*, *33*, 555–567.

Helson, H. (1964). *Adaptation level theory*. New York: Harper & Row.

Horn, B. K. P. (1974). Determining lightness from an image. *Computer Graphics and Image Processing*, *3*, 277–299.

Hurlbert, A. [C.] (1986). Formal connections between lightness algorithms. *Journal of the Optical Society of America A*, *3*, 1684–1693.

Hurlbert, A. C., & Poggio, T. A. (1988). Synthesizing a color algorithm from examples. *Science*, *239*, 482–485.

Jacobsen, A., & Gilchrist, A. (1988). The ratio principle holds over a million-to-one range of illumination. *Perception and Psychophysics*, *43*, 1–6.

Judd, D. B. (1940). Hue saturation and lightness of surface colors with chromatic illumination. *Journal of the Optical Society of America*, *30*, 2–32.

Katz, D. (1935). *The world of colour*. London: Kegan Paul, Trench, Trubner.

Koffka, K. (1935). *Principles of gestalt psychology*. New York: Harcourt, Brace, & World.

Land, E. [H.] (1977). The Retinex theory of color vision. *Scientific American*, *237*, 108–128.

Land, E. [H.] (1986). Recent advances in Retinex theory. *Vision Research*, *26*, 7–22.

Land, E. [H.], Hubel, D. H., Livingstone, M. S., Perry, S. H., & Burns, M. M. (1983). Colour-generating interactions across the corpus callosum. *Nature*, *303*, 616–618.

Land, E. H., & McCann, J. J. (1971). Lightness and retinex theory. *Journal of the Optical Society of America*, *61*, 1–11.

Li, X., & Gilchrist, A. L. (1993). Geometric configuration and anchoring of surface lightness. *Investigative Ophthalmology and Visual Science*, *34*(Suppl.), 748.

Mach, E. (1865). On the effect of the spatial distribution of the light stimulus on the retina. In F. Ratliff, *Mach bands*: *quantitative studies on neural networks in the retina* (pp. 253–271). San Francisco: Holden-Day.

McCann, J. J. (1989). The role of simple nonlinear operations in modeling human lightness and color sensations. *SPIE Proceedings*, *1077*, 355–363.

McCann, J. J. (1992). Rules for colour constancy. *Ophthalmological and Physiological Optics*, *12*, 175–177.

Melfi, T. O., & Schirillo, J. A. (2000). T-junctions in inhomogeneous surrounds. *Vision Research*, *40*, 3735–3741.

Müller, G. E. (1896). Zur psychophysik der gesichtsempfindungen. *Zeitschrift für Psychologie*, *10*, 1–81.

Paradiso, M. A., & Nakayama, K. (1991). Brightness perception and filling-in. *Vision Research*, *31*, 1221–1236.

Paradiso, M. A., & Hahn, S. (1996). Filling-in percepts produced by luminance modulation. *Vision Research*, *36*, 2657–2663.

Ratliff, F. (1965). *Mach bands*: *quantitative studies on neural networks in the retina*. San Francisco: Holden-Day.

Reid, R. C., & Shapley, R. (1988). Brightness induction by local contrast and the spatial dependence of assimilation. *Vision Research*, *28*, 115–132.

Rossi, A. F., & Paradiso, M. A. (1996). Temporal limits of brightness induction and mechanisms of brightness perception. *Vision Research*, *36*, 1391–1398.

Rossi, A. F., Rittenhouse, C. D., & Paradiso, M. A. (1996). The representation of brightness in primary visual cortex. *Science*, *273*, 1104–1107.

Rudd, M. E. (2000). Psychophysical evidence for lightness computation by a neural filling-in mechanism. *Abstracts of the Psychonomic Society*, *5*, 87.

Rudd, M. E. (2001). Lightness computation by a neural filling-in mechanism. *Proceedings of the Society of Photo-Optical Instrumentation Engineers: Human Vision and Electronic Imaging VI*, 410–413.

Rudd, M. E., & Arrington, K. F. (2000). Filling-in of surface darkness. *Investigative Ophthalmology and Visual Science*, *41*(Suppl.), S226.

Schirillo, J. A. (1999a). Surround articulation. I. Brightness judgments. *Journal of the Optical Society of America A*, *16*, 793–803.

Schirillo, J. A. (1999b). Surround articulation. II. Lightness judgments. *Journal of the Optical Society of America A*, *16*, 804–811.

Schirillo, J. A., Reeves, A., & Arend, L. (1990). Perceived lightness, but not brightness, of achromatic surfaces depends on perceived depth information. *Perception and Psychophysics*, *48*, 82–90.

Schirillo, J. A., & Shevell, S. K. (1993). Lightness and brightness judgments of coplanar retinally non-contiguous surfaces. *Journal of the Optical Society of America A*, *10*, 2442–2452.

Schirillo, J. A., & Shevell, S. K. (1996). Brightness contrast from inhomogeneous surrounds. *Vision Research*, *36*, 1783–1796.

Shapley, R., & Reid, R. C. (1985). Contrast and assimilation in the perception of brightness. *Proceedings of the National Academy of Sciences USA*, *82*, 5983–5986.

Todorović, D. (1997). Lightness and junctions. *Perception*, *26*, 379–394.

Wallach, H. (1948). Brightness constancy and the nature of achromatic colors. *Journal of Experimental Psychology*, *38*, 310–312.

Wallach, H. (1976). *On perception*. New York: Quadrangle.

Whittle, P., & Challands, P. D. C. (1969). The effect of background luminance on the brightness of flashes. *Vision Research*, *9*, 1095–1110.

Wolff, W. (1933). Concerning the contrast-causing effect of transformed colors. *Psychologische Forschung*, *18*, 90–97.